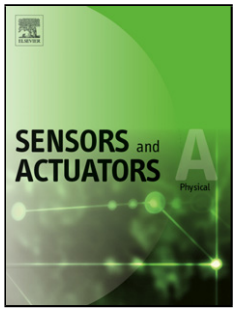

Title: Dynamic Characterization of a Low Cost Microwave Water-Cut Sensor in a Flow Loop

Authors: Muhammad Akram Karimi, Muhammad Arsalan, Atif Shamim

PII: S0924-4247(16)30720-8
DOI: http://dx.doi.org/doi:10.1016/j.sna.2017.03.016
Reference: SNA 10030

To appear in: *Sensors and Actuators A*

Received date: 17-10-2016
Revised date: 5-3-2017
Accepted date: 11-3-2017

Please cite this article as: Muhammad Akram Karimi, Muhammad Arsalan, Atif Shamim, Dynamic Characterization of a Low Cost Microwave Water-Cut Sensor in a Flow Loop, Sensors and Actuators: A Physicalhttp://dx.doi.org/10.1016/j.sna.2017.03.016

Dynamic Characterization of a Low Cost Microwave Water-Cut Sensor in a Flow Loop

Muhammad Akram Karimi[1], Muhammad Arsalan[2], Atif Shamim[1]

1. Authors are with Integrated Microwave Packaging Antennas and Circuits Technology (IMPACT), at the Computer, Electrical, and Mathematical Sciences and Engineering Division, King Abdullah University of Science and Technology, 4700 KAUST, 23955 Thuwal, Kingdom of Saudi Arabia (corresponding email: muhammadakram.karimi@kaust.edu.sa)
2. Author is with EXPEC ARC, Production Technology Team in Saudi Aramco, Kingdom of Saudi Arabia (muhammad.arsalan@aramco.com)

Highlights

- A low cost, non-intrusive and full-range microwave water-cut sensor has been characterized in a custom designed flow loop
- Performance of the water cut sensor has been tested by installing it in horizontal as well as in vertical orientations
- Flow rate effect on the performance of the sensor has been thoroughly investigated

***Abstract*—Inline precise measurement of water fraction in oil (i.e. water-cut [WC]) finds numerous applications in oil and gas industry. This paper presents the characterization of an extremely low cost, completely non-intrusive and full range microwave water-cut sensor based upon pipe conformable microwave T-resonator. A 10″ microwave stub based T-resonator has been implemented directly on the pipe surface whose resonance frequency changes in the frequency band of 90MHz-190MHz (111%) with changing water fraction in oil. The designed sensor is capable of detecting even small changes in WC with a resolution of 0.07% at low WC and 0.5%WC at high WC. The performance of the microwave WC sensor has been tested in an in-house flow loop. The proposed WC sensor has been characterized over full water-cut range (0% to 100%) not only in vertical but also in horizontal orientation. The sensor has shown predictable response in both orientations with huge frequency shift. Moreover, flow rate effect has also been investigated on the proposed WC sensor's performance and it has been found that the sensor's repeatability is within 2.5% WC for variable flow rates.**

***Index Terms*—Water-cut, Microwave Sensor, Flow Loop**

I. Introduction

WATERCUT (WC) measurement (measuring volumetric fraction of water in oil) is crucial in oil industry for multiple purposes including reservoir management, production allocation and flow assurance. The most prevalent way to measure WC is to measure dielectric properties of oil/water (O/W) mixture. Studies have shown that measuring dielectric properties of O/W mixture at higher frequencies (tens of MHz) provides much higher sensitivity compared to lower frequencies (few kHz) over full range of WC [1] [2]. Microwave transmission or microwave resonance based WC sensors provide a way to measure dielectric constant at high excitation frequency. Researchers have used a microfluidic channel based WC sensor using a T-resonator [3] but it can't be used for inline WC detection. Microwave transmission based WC sensors suffer from high loss in presence of -saline water (high conductive losses) while microwave resonance (mostly cavity resonance) based WC sensors are either intrusive in nature [4] [5] or have shown very less sensitivity of only 1% [6, 7]. Water fraction in air has been detected intrusively by observing shift in resonance frequency of a monopole antenna [8]. Flat microstrip resonators have been used to detect the level or particle composition of oil/.water mixtures [9] [10] [11]. Unlike intrusive or planar oil/water characterization methods, this work presents a pipe conformable and completely non-intrusive microwave T-resonator as a WC sensor.

This work focuses on dynamic flow loop characterization of a novel microwave WC sensor implemented directly on the pipe surface. Flow loop is a laboratory test setup which is used to mimic the flow conditions as experienced in the oil field. Studies have shown that flow loop helps building the behavioral model and look-up table for the water hold-up sensor which are later

used in its field testing [12]. Flow loop characterization is a step before taking the sensor for the field testing [13].

This paper explains the construction of a basic 2-phase (oil, water) flow loop which was used to characterize the novel microwave resonator based water-cut sensor. The resonance frequency of the sensor is shifted with water fraction and is measured using a vector network analyzer (VNA). Most of previous work has been done on static oil, water and air [9] [10] [6] [11] while limited literature addresses the dynamic characterization of air/water mixtures which is available only for vertical orientation [7] [14]. In this work we have characterized the sensor in vertical as well as in horizontal installation which are essential in recent proliferation of multi-lateral wells [15].

Next section briefly covers the design of the novel microwave resonator based WC sensor while section 3 discusses about the construction of the flow loop which was used to characterize the proposed WC sensor under different flow conditions presented in section 4.

II. Design, fabrication and static characterization

Oil and water differ in their dielectric properties and microstrip based T-resonator provides a way to measure dielectric properties of the substrates. The proposed WC sensor is also based upon the principle of T-resonance. Detailed description of the proposed WC sensor can be found in [16] which is summarized herein for the sake of completeness.

A. Design

Unlike conventional T-resonators, which are implemented on the flat substrates having fixed dielectric properties [17], our proposed T-resonator (shown in Figure 1) has been implemented directly on the outer surface of 3D pipe containing fluids of different dielectric properties depending upon the water fraction in oil. Similar to typical T-resonators, it also consists of a feedline (FL), a λ/4 open stub (on upper pipe surface) and a ground plane (on bottom pipe surface). Standard 50Ω FL is usually made on an unvarying substrate because its impedance may alter with the dielectric properties of the substrate. The challenge in implementing T-resonator on pipe surface was to isolate the FL from the varying dielectric properties of oil/water mixture inside the pipe. In order to isolate FL from the effects of variable fluid inside the pipe, we are proposing to extend the bottom ground plane to the top in the form of a ring which runs underneath the FL. This way, impedance of FL is not affected by the varying fluid mixtures inside the pipe and can easily be matched to 50Ω as desired. FL and its corresponding ring ground are separated using a dielectric separator. In contrast to FL, impedance of shunt stub varies with varying
relative fraction of oil and water inside the pipe because its corresponding ground lies underneath the pipe surface. The varying impedance of the shunt stub results in the shift in resonance frequency of the T-resonator. The sensor implemented on top of acrylic pipe surface has been simulated in the electromagnetic simulator Ansys HFSS. Simulated results along with the measurements have been presented in section IV. The physical dimensions of the sensor have been summarized in Table 1.

B. Fabrication

The WC sensor has been realized using extremely low cost method of copper taping. Most of the design can be realized using standard copper tape. The FL was precisely cut using a laser diode (manufactured by Universal Laser Systems) with maximum output power of 1mW at the wavelength of 630-680nm. The precise dimension of FL helps achieving better matching of the T-resonator with measurement equipment. The fabrication process has been summarized in Figure 2.

It's evident from Figure 2 that the presented design cannot be directly applied on the metallic pipes. But with the passage of time, non-metallic pipes made of high temperature and high pressure tolerant materials like Polyether ether ketone (PEEK) and glass fiber are becoming attractive to be used in oil and gas industry because they offer longer operational life due to their ability to resist to corrosion. Few industrial WC sensors like Krohne M-PHASE5000 are already using non-metallic lining [18] inside a metallic enclosure. Such non-metallic materials can be used to realize our proposed design for industrial applications.

C. Static Characterization

At low flow rates and horizontal pipe orientation, oil and water mixture experiences stratified flow regime in which light liquid (oil) floats on top of heavy liquid (water) [19]. This scenario resembles the case when oil and water are kept statically inside the pipe. For initial verification of our design, we characterized our sensor in this static scenario with a step change of 10% WC both in simulations and measurements. As an example, the cross sectional view of the pipe for the case of 20% WC has been shown in inset of Figure 3. The resonant frequency of the T-resonator shifts down with increasing water fraction [3] which in our case has been plotted against WC in Figure 3. As evident from the figure that the simulated and measured responses show the similar trend. The constant shift in measured response compared to simulations can be explained with the possible discrepancy in dielectric properties of acrylic pipe used in the simulations.

III. Flow Loop Measurement Setup

In order to verify the applicability of the designed WC sensor under the scenario of moving oil/water mixtures in the pipelines, a basic flow loop was constructed. The response of the designed sensor was measured in the horizontal as well as in the vertical orientations in the flow loop. The qualitative effect of the mixture's speed on the response of the sensor was also investigated.

A. Design of basic flow loop

The flow loop was intended to provide the following basic capabilities:

1. Circulation of known fractions of oil/water mixture;
2. Electrical and manual capability to adjust the flow rate;
3. Removable vertical and horizontal test sections; and
4. Capability of easy adjustment of the WC;

Keeping in mind the above-mentioned capabilities, a design was finalized which contained two parts:

1. Main circulation piping on a wooden support (lies in Z-X plane as shown in Figure 4); and
2. An area behind the wooden support containing the reservoir and pump (lies in X-Y plane as shown in Figure 5.

In the main circulation loop, shown in Figure 4, the gray pipe is made of PVC, while the transparent pipe is acrylic-based. The reservoir, containing oil/water mixture, is contained on the back side of the main circulation loop. The mixture is pumped into the main circulation loop from point 1 and exits from point 2 back into the reservoir. As points 1 and 2 have 90° PVC bends which cause turbulence in the flow, the vertical test section is placed at a distance of approximately 10 ft. from point 1to allow the mixture to get settled. A dispersed bubble regime is observed in the vertical test section [19]. In contrast to the vertical test section, horizontal test section is located just 1 ft. from the 90° bend due to the space constraints in the horizontal direction. Consequently, the horizontal test section experiences a high degree of turbulence which results in stratified wavy or plug/slug flow depending upon the WC and flow rate [19].

The effect of these flow regimes on the performance of the WC sensor will be discussed in the following sections. It can also be seen from Figure 4 that the test sections are removable with the help of attached PVC flanges. The test sections have been made with transparent acrylic pipe of 50mm diameter in order to visually observe the flow regimes. Since the return path is not critical in these experiments, so it is made with smaller diameter (25.4mm) PVC pipe to minimize the overall pipe volume of the flow loop. This enables experiments with minimum volume of the fluid.

The back side (X-Y plane) of the main circulation loop is shown in Figure 5, which contains the following items:

1. Acrylic tank/reservoir (for keeping known amounts of oil/water to achieve different WCs);
2. Centrifugal pump for pumping the mixture into the flow loop;
3. Bypass valve to manually reduce the flow rate
4. Drainage valve to drain the fluid out of acrylic tank

Since the volume of the acrylic tank is limited, the returning fluid (oil and water mixture) does not have enough time to get separated and thus oil and water pass through the flow loop in the form of an emulsion as a single liquid phase. At higher WC, oil phase (dispersed phase[1]) get dispersed in the water phase (continuous phase) while opposite is true for low WC. The flow rate is electrically adjusted with the help of Variable Frequency Drive (VFD) by varying the input frequency of AC motor installed in the centrifugal pump. Flow rate of the oil/water emulsion is directly proportional to the frequency of VFD.

IV. Simulations and WC sensor Characterization

In order to predict the response of the designed WC sensor, HFSS simulations have been carried out on the pipe structure filled with different volumetric fractions of oil and water in the form of homogenous emulsion. The dielectric properties of all the materials used in the design of WC sensor have been obtained from the literature [16] [20]. Figure 6 shows the dielectric properties of the oil/water emulsions at the operational frequency of the sensor. Simulated results have been plotted with measured response of the sensor in the vertical and horizontal sections of the flow loop as shown in Figure 8 and Figure 10.

In order to measure the response of the WC sensor in the designed flow loop, acrylic reservoir tank as shown in Figure 5, is filled with particular fraction of vegetable corn flower oil and tap water. Oil and water are made to flow in the flow loop with the help of the centrifugal pump. The typical flow rate provided by 1 horse power (hp) centrifugal pump at 50 Hz is around 500-600L/min which is high enough to thoroughly mix oil and water and form a homogenous emulsion [21]. The typical viscosity of

[1] Dispersed phase is the phase which is dispersed in continuous phase (carrier for small particles) in the form of small particles.

corn flower oil is 65 cP, while room-temperature water (20°C) has a viscosity of 1 cP [22]. The effective viscosity of oil/water emulsion decreases by increasing the water content (or WC). The change in viscosity

of emulsion can impact the flow patterns in the pipe which will be explained later in this section.

Since the flow regimes are different in the vertical and horizontal sections of the flow loop, the dynamic measurements have been divided into two categories.

A. WC sensor's response in vertical orientation

It can be observed in Figure 4 that the oil/water emulsion will flow against the gravity in the vertical test section. Since the gravitational force acting on the cross sectional area of test section is constant and only one liquid phase (oil/water emulsion) is being injected in the loop, it is expected that this liquid phase will acquire the whole cross section of the tube. Since this liquid phase is an emulsion, we can correlate the flow pattern in the vertical section to the "Bubble flow regime" [19], as shown in the inset of Figure 8. The transmission coefficient (S_{21}) response of the WC sensor (shown in Figure 7) has been measured using a handheld VNA against the full range of WC (0-100 %, with a step of 10%).

The percentage shift in resonant frequency for full range of WC (0-100%) is almost 116% i.e. resonant frequency shifts from 195MHz-90MHz. The proposed WC sensor is sensitive enough to cover the full range of WC, though the sensitivity is non-linear owing to its higher frequency shift at lower WCs compared to higher WCs. The designed sensor gives a resolution of 0.07% at low WC and 0.5%WC at high WC with the Fieldfox VNA.

It must be noted that the microwaves travel at the speed of $(3*108/\sqrt{\quad})$ where εeff is the effective dielectric constant of the medium so the sensor must respond in the order of fraction of a micro second. The main delay comes from the measurement instrument and its settings which in our case is VNA with 601 number of points, 30kHz IF bandwidth and 10 point averaging and results into a span time of 0.4 sec. The response time of the sensor can significantly be improved by utilizing a customized readout circuitry based upon the microwave oscillator.

In order to investigate the effect of the flow rate on the performance of the sensor, S_{21} response over full WC range has been measured for three different frequencies of VFD i.e. 40, 50 and 60 Hz which correspond to low, medium and high flow rates respectively. Since the sensing principle is to detect the resonant frequency, so we extracted the resonant frequency from S_{21} response and plotted it against the WC for 3 different flow rates as shown in Figure 8. Simulated response curve is shown in black in Figure 8.

As evident from Figure 8, response of WC sensor is not much affected by the flow rate because the flow regime is not changed. The sensor's repeatability for different flow rates is within 2.5% WC which has been calculated using average range method [23]. The sharp bend in the response from 50% to 60% WC is due to the change of continuous phase into dispersed phase [24].

Figure 8 shows that the simulations show similar trend as observed by the measurements, which confirms the simulation model. However, there exists a slight offset as compared to the measurements. This offset is most likely due to slight variation in the dielectric properties of the materials used in the construction of the sensor. Moreover, small quantity of non-conductive epoxy has been used for water-proof sealing of the SMA connector which has not been considered in simulations. These factors may account for slight offset of the simulations with that of the measurements. These small discrepancies between simulation and measurements can easily be calibrated out while performing real measurements which will eventually be compared with the measured characterized curves.

Nonetheless, the proposed sensor has been shown to be sufficiently sensitive over full range of WC. The consistent performance of the sensor over different flow rates not only proves that the sensor is insensitive to the flow rate but also depicts its repeatability.

B. WC sensor's response in a horizontal orientation

The horizontal section, shown in Figure 4, is very close to 90° bend which can become a cause of significant turbulence in this test section. A study done in [10-11] employed perturbation methods to investigate the flow in curved channels, reporting that flow in the core of the pipe moves quickly and is forced outwards from the center of the curvature by centrifugal force. In contrast, fluid close to the walls is pushed towards the inside because of the pressure difference caused by the difference in the speed of the streamlines. This intermingling of the streamlines downstream of 90° bend is the cause for the fluid to be unable to sweep the complete air out of the horizontal test section. That is why air (gas phase) becomes part of the oil/water emulsion (liquid phase) in this test section.

Similar to vertical section, the transmission coefficient (S_{21}) response of the WC sensor (shown in Figure 9) has been measured using a handheld VNA against the full range of WC (0-100 %, with a step of 10%).

The percentage shift in the resonant frequency in this case is almost 105% as the absolute resonant frequency shifts from 195MHz to 95 MHz while changing the WC from 0% to 100%. Similar to the vertical section, sensor shows more sensitivity at lower WC than at higher WC.

Effect of flow rate on the response of horizontal test section has also been investigated at three different frequencies of VFD i.e. 40, 50 and 60Hz which correspond to low, medium and high flow rates respectively. Similar to the previous case, resonance frequencies have been extracted from S_{21} responses and are plotted against the WC for three different flow rates as shown in Figure 10. Simulated curve, shown in black color, is also the part of Figure 10.

It is evident from Figure 10 that the horizontal section of the WC sensor shows almost the same sensitivity and frequency range as depicted by vertical section (Figure 8). This is particularly true at low WC where relatively less air becomes the part of the oil/water mixture. High WC and high flow rate favor more air (ε_r=1) to get trapped with oil/water mixture (ε_r=2.2 to ε_r=80) which changes the effective dielectric constant (ε_{eff}) measured by the T-resonator. It results in slight deviation in horizontal section's response compared to the vertical one at high WC. This deviation is directly linked with the percentage of air (caused by the fluid turbulence) introduced with oil/water mixture. Simulations show the similar trend as shown by measurements except for some offset similar to the vertical case.

The Reynolds number[2] is a measure of turbulence in the flow which is given by the following equation:

$$= \frac{\quad}{\quad} \qquad (1)$$

Where "D" is the characteristic length which remains the same in horizontal test section. It means that the turbulence is directly proportional to density " ", velocity "v" of the emulsion and inversely proportional to its viscosity "μ". It means that one should expect high speed and high WC (less viscous) mixture to be more turbulent and hence more deviating from ideal response. Figure 10 conveys the same information in which we can see that the deviation is maximum at higher WC and higher flow rate (corresponding to 60 Hz frequency of VFD) because more air becomes part of the mixture. Since the air fraction varies periodically with time, we have applied 50 point averaging (instead of 10 point averaging used in vertical case) on VNA to average the time variation because of air fraction while getting the S_{21} response shown in Figure 9.

However, it is worth mentioning here that WC sensor senses the relative fraction of oil and water in a mixture of oil/water only. There are some other methods to measure the gas fraction which are integrated with the WC sensor to sense the three phases independently.

It must be mentioned here that all the measurements presented in this work have been conducted on room temperature (25° C) but the temperature can be much higher than this in real oil production facility. Higher temperature results into more loss or deterioration in the quality factor of the resonator but the resonant frequency can still easily be extracted [16].

V. Comparison with commercial WC sensors

Although commercially available WC sensors are quite sophisticated which make them bulky and expensive as well but their resolution is comparable to our sensor which is extremely low cost, light weight and fully non-intrusive. Table 2 enlists the resolution of some of commercially available WC sensors.

As can be seen from Table 2 that that the resolution of commercially available WC sensors varies from ±0.01% WC to ±2% WC. While our designed sensor gives a resolution of 0.07% at low WC and 0.5%WC at high WC. Accuracy of the proposed sensor can be compared with the commercial ones after performing measurements on random WC values in the real field environment. This can be done as part of the future work.

VI. Conclusion

This work presents the construction of a basic flow loop and dynamic characterization of a novel low cost and pipe conformal WC sensor for the first time. The sensor performs equally well in vertical as well in horizontal orientations with achieved sensitivity of more than 105% in both the cases. Proposed WC sensor performs equally well under all flow rate conditions with slight deviations at high WC and high flow rate in case of horizontal test section due to the limitations of flow loop test setup. In future, the proposed WC sensor can be tested in more sophisticated flow loop to test its performance in more flow patterns. Eventually the proposed T-resonator based WC sensor will be integrated with a microwave oscillator to eliminate the need of use of VNA to record its response. Afterwards, the design will be ready to be tested in the field as a standalone and self-contained WC sensor.

[2] Reynolds number is a dimensionless ratio of inertial to viscous forces of the flow which describes whether the flow conditions lead to laminar or turbulent flow.

VII. REFERENCES

[1] M. Demori, "A capacitive sensor system for the analysis of two-phase flows of oil and conductive water," *Sensors and Actuators A: Physical*, vol. 163, no. 1, pp. 172-179, 2010.

[2] A. S. M. B. W.Q. Yang, "High frequency and high resolution capacitance measuring circuit for process tomography," *IEE Proceedings-Circuits, Devices and Systems*, vol. 141, no. 3, pp. 215 - 219, 1994.

[3] D. C. C. F. S. G. McKerricher, "Crude oil WC sensing with disposable laser ablated and inkjet printed RF microfluidics," in *IMS*, 2014.

[4] E. G. Nyfors, "CYLINDRICAL MICROWAVE RESONATOR SENSORS FOR MEASURING MATERIALS UNDER FLOW," Helsinki University of Technology, Espoo, 2000.

[5] L. Y. F. H. Hongfu Guo, "A cylindrical cavity sensor for liquid water content measurement," *Sensors and Actuators A: Physical*, vol. 236, pp. 133-139, 2016.

[6] M. A. A. S. A. A.-S. S. K. A. B. C.S. Oon, "Experimental study on a feasibility of using electromagnetic wave cylindrical cavity sensor to monitor the percentage of water fraction in a two phase system," *Sensors and Actuators A: Physical*, p. 140–149, 2016.

[7] "Detection of the gas–liquid two-phase flow regimes using non-intrusive microwave cylindrical cavity sensor," *Journal of Electromagnetic Waves and Applications*, pp. 2241-2255, 2016.

[8] A. O. H. A. a. M. C. Hesham Enshasy, "Microwave NDT for in situ monitoring of fresh/saline water fraction in natural gas flow," *INTERNATIONAL JOURNAL OF ELECTRONICS*, 2016.

[9] X. Y. D. B. A. P. Ali Abduljabar, "Microstrip Split Ring Resonator for Microsphere Detection and Characterization," in *International Microwave Symposium (IMS)-2015*, 2015.

[10] M. D. resonatorMohammad Hossein Zarifi, "Liquid sensing in aquatic environment using high quality planarmicrowave resonator," *Sensors and Actuators B: Chemical*, p. 517–521, 2015.

[11] P. S. M. A. Z. H. M. D. Mohammad H. Zarifi, "Particle size characterization using a high resolution planar resonatorsensor in a lossy medium," *Sensors and Actuators B: Chemical*, p. 332–337, 2016.

[12] J. H. ,. F. S. ,. B. C. ,. X. S. &. Q. C. Xingbin Liu, "Conductance sensor for measurement of the fluid water cut and flow rate in production wells," *Chemical Engineering Communications*, vol. 197, no. 2, pp. 232-238, 2009.

[13] DNV.GL, "DNV GL Groningen Multiphase Flow Laboratory," DNV.GL, [Online]. Available: https://www.dnvgl.com/oilgas/laboratories-test-sites/groningen-multiphase-flow-laboratory.html.

[14] H. Y.-F. R. Y.-Y. Z. L.-S. a. J. N.-D. Zhao An, "Ultrasonic method for measuring water holdup of low velocity and high-water-cut oil-water two-phase flow," *Applied Geophysics*, vol. 13, pp. 179-193, 2016.

[15] D. J. Xiao, "Determining Water Volume Fraction for Oil-Water Production with Speed of Sound Measurement," *Saudi Aramco Journal of Technology*, Summer 2015.

[16] M. A. A. S. Muhammad Akram Karimi, "Low cost and pipe conformable microwave based water-cut sensor," *IEEE Sensors*, no. 99, 2016.

[17] M. K. J.-P. S. ,. P. S. K. -P. Latti, "A Review of Microstrip T-Resonator Method in Determining the Dielectric Properties of Printed Circuit Board Materials," *IEEE Transactions on Instrumentation and Measurement*, vol. 56, no. 5, pp. 1845 - 1850 , 2007.

[18] K. N. T. B.V., "M-Phase 5000," 2015. [Online]. Available: cdn.krohne.com/dic/FL_M-PHASE5000_en_160113.pdf.

[19] U. D. ChemWiki, "Co–Current Flow," [Online]. Available: http://chemwiki.ucdavis.edu/Under_Construction/EngineeringWiki/Fluid_Mechanics/13%3A_Multi%E2%80%93Phase_Flow/13.5%3A_Classification_of_Liquid-Liquid_Flow_Regimes/13.5.1%3A_Co%E2%80%93Current_Flow.

[20] HyperPhysics, "Dielectric Constants at 20°C".

[21] PEDROLLO, "vip-tehnika," [Online]. Available: www.vip-tehnika.si/produkti/pedrollo/pdf/pedrollo-hf-medium-50hz.pdf.

[22] T. P. Hypertextbook, "Viscosity," [Online]. Available: http://physics.info/viscosity/.

[23] A. Milivojevich, "How to Calculate Gage Repeatability Using the Average Range," [Online]. Available: https://andrewmilivojevich.com/how-to-calculate-gage-repeatability-using-the-average-range/.

[24] K. H. Ngan, "Phase Inversion in dispersed liquid-liquid pipe flow," in *PhD Thesis* , London, UCL, 2010, p. 125.

[25] Weatherford, "Red Eye Series of Water-Cut Meters," 2015. [Online]. Available: http://www.weatherford.com/doc/wft297766.

[26] Roxar, "Roxar Watercut meter," 2016. [Online]. Available:

http://www2.emersonprocess.com/siteadmincenter/PM%20Roxar%20Documents/Roxar%20Watercut%20meter%20Data%20Sheet.pdf.

[27] P. Dynamics, "Installation and Instruction Manual-Full Range Water in Hydrocarbon Analyzer," [Online]. Available: http://www.phasedynamics.com/images/Analyzerdocuments/0063-00003-000RevB.pdf.

[28] KAM, "OWD Water Cut Meter," [Online]. Available: http://www.kam.com/kam-products/owd-oil-water-detector/.

[29] D. C. C. F. S. G. McKerricher, "Crude oil WC sensing with disposable laser ablated and inkjet printed RF microfluidics," in *IMS*, 2014.

[30] "Viscosity and Fluid Flow," [Online]. Available: http://wps.aw.com/wps/media/objects/877/898586/topics/topic04.pdf.

[31] W. R. Dean, "Fluid Motion in a Curved Channel," *Proceedings of the Royal Society A*, vol. 121, no. 787, 1928.

[32] W. Dean, "he stream-line motion of fluid in a curved pipe (Second paper)," *Philosophical Magazine and Journal of Science*, vol. 5, no. 30, 1928.

Bibliography

VIII. Muhammad Akram Karimi

Muhammad Akram Karimi received his B. Eng. Degree in electrical engineering with two gold medals from University of Engineering and Technology, Lahore, Pakistan, in 2013. He has been an intern in Mentor Graphics and worked as an embedded system developer in MicroTech industries after his Bachelors. He completed his MS degree from King Abdullah University of Science and Technology (KAUST), Saudi Arabia, in 2015. He holds two patents. He is the recipient of best student paper award at International Microwave Symposium (IMS) in 2016. He is currently pursuing his PhD degree from KAUST and his research interests include microwave sensors for oil & gas and biomedical applications. He is also interested in THz device fabrication, characterization and its applications for imaging.

IX. Muhammad Arsalan

Muhammad Arsalan received the BSc degree from the University of Karachi, Karachi, Pakistan, in 1995, the BE degree from Institute of Industrial Electronics Engineering (IIEE), NED University of Engineering and Technology, Karachi, Pakistan, in 1999, and the MASc and PhD degrees in Electronics Engineering from Carleton University, Ottawa, ON, Canada, in 2004 and 2009, respectively. In 2004, he was an Invited Researcher and Natural Sciences and Engineering Research Council-Japan Society for the Promotion of Science (NSERC-JSPS) Fellow with the Tokyo Institute of Technology. From 2005 to 2008, he was an NSERC Alexander Graham Bell Graduate Scholar with Carleton University. From 2009 to 2010, he was a National Aeronautics and Space Administration (NASA) Postdoctoral Fellow with the University of Maine. In 2010, he joined the King Abdullah University of Science and Technology (KAUST), Thuwal, Saudi Arabia, as an NSERC Postdoctoral Research Fellow. Since 2013, he is with The Exploration and Petroleum Engineering Center - Advanced Research Center (EXPEC - ARC) of Saudi Aramco. His research interests are in developing wireless sensor systems using low-power mixed-signal application specific integrated circuits (ASICs), micro and nano-sensors, on-chip antennas, RFICs, and energy harvesting. Dr. Arsalan was the recipient of a number of academic, research, and entrepreneurial awards for his research and innovations including the Information Technology Association of Canada (ITAC) Strategic Microelectronics Council (SMC) Award of the Canadian Microelectronics Corporation TEXPO 2007, the Ottawa Centre of Research Innovation (OCRI) Researcher of the Year Award 2008, the OCRI Entrepreneur of the Year Award 2010, the Enterprize Canada Entrepreneurial Award 2009, and the NSERC Innovation Challenge Award 2010.

X. Atif Shamim

Atif Shamim (SM'13) received the M.A.Sc. and Ph.D. degrees in electrical engineering from Carleton University, Ottawa, ON, Canada, in 2004 and 2009, respectively. From 2007 to 2009, he was a Natural Scientific and Engineering Research Council (NSERC) of Canada Alexander Graham Bell Graduate Scholar with Carleton University. In 2009, he was an NSERC Postdoctoral Fellow with the Royal Military College Canada. In 2010, he joined the Electrical Engineering Program, King Abdullah University of Science and Technology (KAUST), where he is currently an Assistant Professor and Principal Investigator with the IMPACT Laboratory.

In 2006, he was an Invited Researcher with the VTT Micro-modules Research Center, Oulu, Finland. He has authored or coauthored over 100 international publications. He holds 13 patents. His research interests are integrated on-chip antennas, low-power CMOS RF integrated circuits (RFICs) for system-on-chip (SoC) applications and advanced system-on-package (SoP) designs in multilayer low-temperature co-fired ceramic (LTCC), liquid crystal polymer (LCP), and paper substrates through screen and inkjet printing techniques. Dr. Shamim serves on the Editorial Board of the IEEE Transactions on Antennas and Propagation. He is the founding chair of the IEEE Microwave Theory and Techniques Society (IEEE MTT-S) and Antennas and Propagation Society (AP-S) Joint Chapter for Western Saudi Arabia. He was the recipient of the Best Paper Prize at the European Microwave Association Conference in 2008. He was the recipient of the 2008 Ottawa Centre of Research Innovation (OCRI), Researcher of the Year Award in Canada. His research on the wireless dosimeter was bestowed the ITAC SMC Award of Canadian Microelectronics Corporation TEXPO in 2007. He was the recipient of the Best Student Paper Finalist Prize of the IEEE AP-S Conference in 2005. He has also been the recipient of numerous business-related awards, including First Prize in Canada's National Business Plan Competition. He was selected for the OCRI Entrepreneur of the Year Award in 2010.

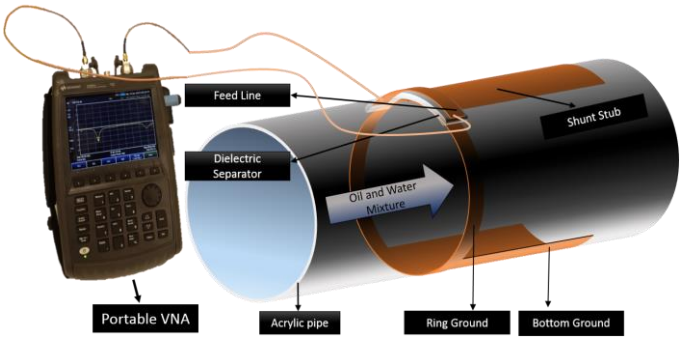

Figure 1. Pipe conformable T-resonator (used as WC sensor) along with portable VNA to extract its transmission coefficients

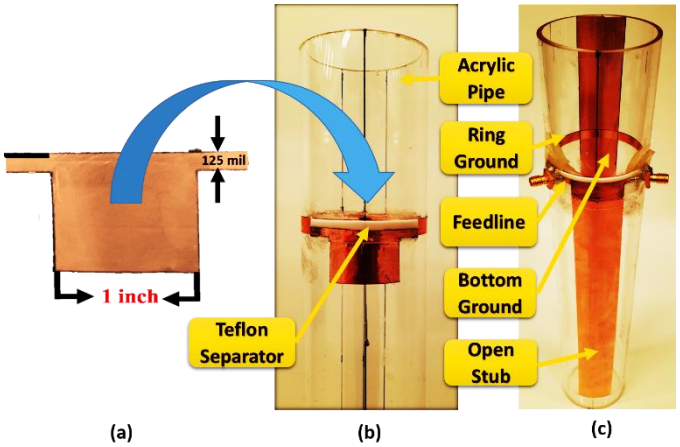

Figure 2. (a) Laser-cut feedline (and partial stub length) (b) acrylic pipe with teflon piece separating the feedline and its corresponding ring-ground (c) complete fabricated prototype with bottom ground plane, open stub and SMA connectors to charcaterize the sensor using Vector Network Analyzer

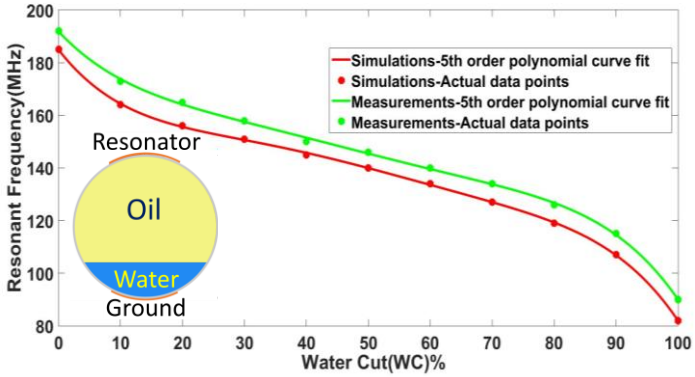

Figure 3. Simulated and measured responses of WC sensor. Inset picture shows the cross sectional view of pipe in this (static) characterization scenario

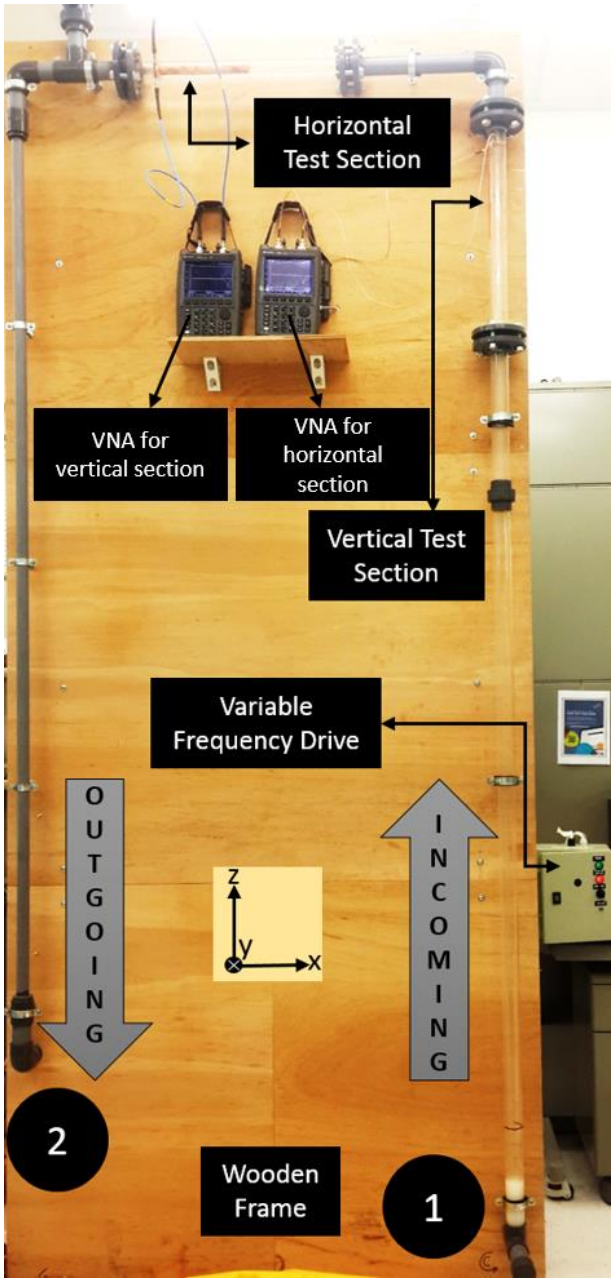

Figure 4. Front side of the flow loop (Main circulation piping on the wooden frame)

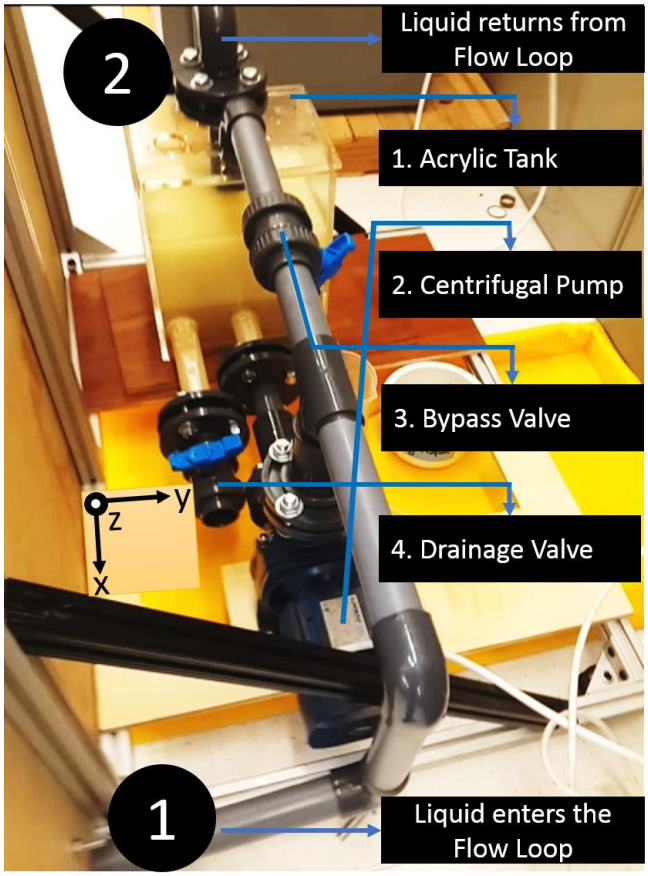

Figure 5. Back side of the flow loop

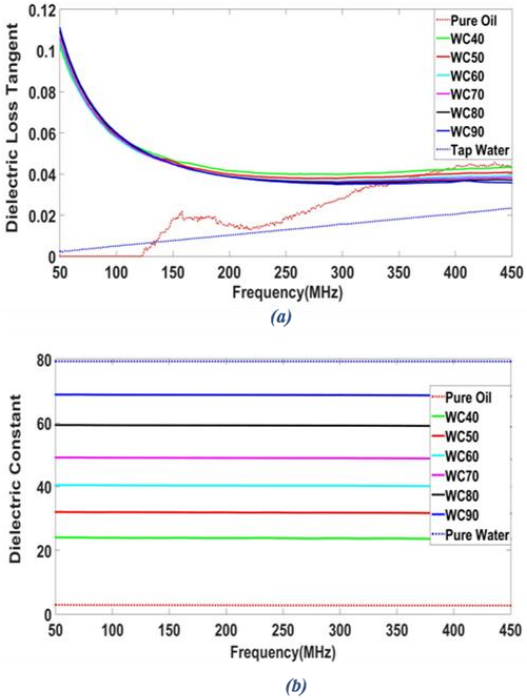

Figure 6. (a) Measured dielectric loss tangent and (b) dielectric constant of oil, water mixtures of different WCs [10]

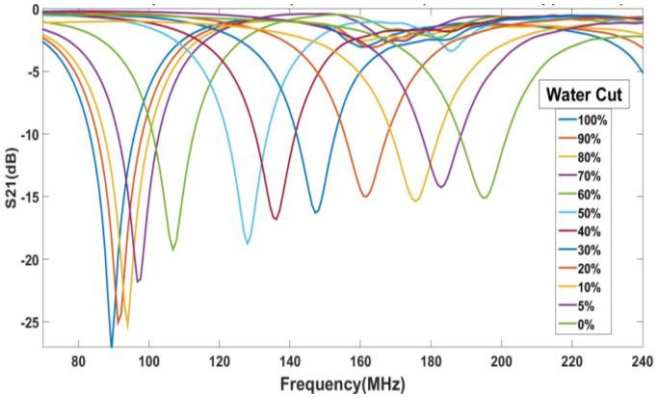

Figure 7. Measured response of WC sensor in vertical orientation at low flow rate (40Hz freq. of VFD)

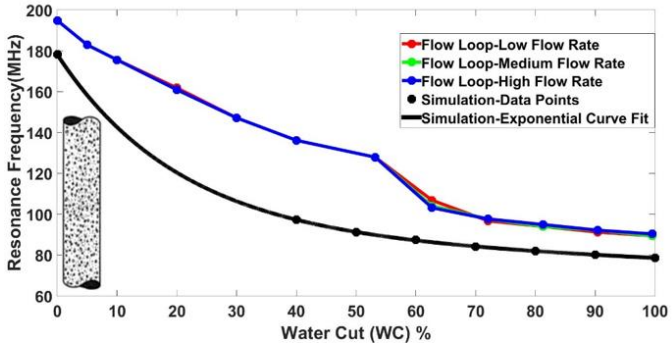

Figure 8. Measured response of WC sensor in vertical orientation at three different flow rates along with simulated curve. Inset shows the dispersed flow regime observed in vertical tests section

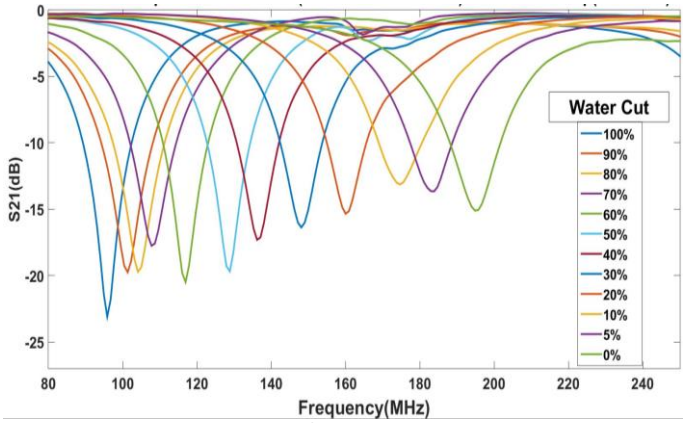

Figure 9. Measured response of WC sensor in horizontal orientation at low flow rate (40Hz freq. of VFD)

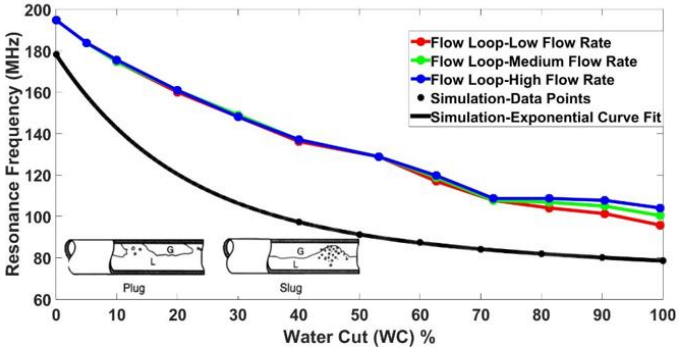

Figure 10. Measured response of WC sensor in horizontal orientation at three different flow rates along with simulated curve. Inset shows the Plug/Slug flow regime observed in horizontal tests section

Table 1. Phsyical dimensions of pipe-conformable WC sensor, simulated in HFSS

Parameter	**Value**	**Reason**
Pipe diameter (D_P)	2″	No size restriction. Design has been validated for pipe diameters up to 8″ diameter with proper scaling
Pipe length (L_P)	14″	To provide enough space to accommodate shunt stub
Length of shunt stub (L_{SS})	10″	Five times the pipe diameter so that most of the field lines could terminate on bottom ground plane instead of terminating nearby ring extension of ground
Width of shunt stub (W_{SS})	1″	To keep the $Z_{0\text{-}SS}$ as close to 50Ω as possible
Separator(ε_r=2.1) Thickness	1mm	To provide reasonable width of FL for 50Ω impedance
Separator Length	2″	Should be larger than width of shunt stub
FL length	2″	FL covers same lateral length as separator does
FL width	0.125″	To provide 50Ω impedance over separator
Width of Ring ground	0.25″	Slightly larger than FL width for proper microstrip mode propagation
Arc length of Bottom ground	22mm	Optimized in HFSS (to give minimum fringing and maximum sensitivity)

Table 2. Comparison of resolution of presented work with commercially available WC sensors

Ref.	**Water Cut meter manufacturer**	**Resolution**
[25]	Weatherford	±2% (with 20% Gas Volume fraction-GVF)
[26]	Roxar	±0.05% (Full Cut Version)
[27]	Phase Dynamics	0.1% (Full Range Version)
[28]	KAM	+/- 0.01%
This work		0.07%-0.5%